Partial discreteness: a new type of prior knowledge for MRI reconstruction

Gabriel Ramos-Llordén[1], Hilde Segers[1], Willem Jan Palenstijn[1], Arnold J. den Dekker[1,2], and Jan Sijbers[1]
[1]*iMinds Vision-Lab, University of Antwerp, Antwerp, Antwerp, Belgium,* [2]*Delft Center for Systems and Control, Delft University of Technology, Delft, Netherlands*

TARGET AUDIENCE: Scientist interested in MRI reconstruction and segmentation.

PURPOSE: In MRI reconstruction, undersampled data sets lead to ill-posed reconstruction problems. To regularize them, prior knowledge is commonly exploited. In this work, we introduce a new type of prior knowledge for ill-posed reconstruction problems where part of the image is assumed to be homogeneous (i.e., can be well represented by a constant magnitude). Examples of MRI applications where partial discreteness can be exploited are MR implants imaging, CSF in spin echo T_2-weighted images, dental MRI with SWIFT sequences or Multiple Sclerosis plaques imaging with FLAIR sequences.

METHOD 1) Partially discrete parametric model: Images that follow the *partial discreteness* assumption are those whose magnitude is composed of a (known) number K of disjoint classes $\mathcal{A}_k$, $k = 1, \dots, K$ representing tissues and background. Some of these classes, $k \in I \subset K$, are assumed to have a constant magnitude ρ_k, but no assumptions on the intensity are made for the rest. An example is shown in Fig. 1, which shows an MRI breast implant image that is represented by three classes ($\mathcal{A}_1, \mathcal{A}_2$ and $\mathcal{A}_3$), of which the background region $\mathcal{A}_1$ and implant region $\mathcal{A}_3$ are assumed to be constant. Such images can be written in parametric form as $\boldsymbol{x}_{dis} = e^{i\boldsymbol{\Phi}} \circ \left(\sum_{k \in I} \boldsymbol{1}_{\mathcal{A}_k} \rho_k + \boldsymbol{x}_{\bar{\mathcal{A}}}\right)$, where $\boldsymbol{\Phi} \in \mathbb{R}^N$ (N is the number of pixels) is the image phase, $\boldsymbol{1}_{\mathcal{A}_k} \in \{0,1\}^N$ is a mask vector for the class $\mathcal{A}_k$, $\mathcal{A} = \bigcup_{k \in I} \mathcal{A}_k$, $\boldsymbol{x}_{\bar{\mathcal{A}}}$ represents the magnitude in classes that do not belong to $\mathcal{A}$ and $\circ$ denotes the Hadamard product.

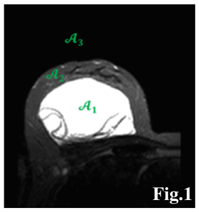

Fig.1

2) l_2 reconstruction with the partial discreteness prior: We formulate the reconstruction problem following the algebraic linear model in a multi-coil acquisition system. K-space data are related to the image $\boldsymbol{x} \in \mathbb{C}^N$ *as* $\boldsymbol{y}_l = \boldsymbol{A}\boldsymbol{x} + \boldsymbol{n}_l$ *with* $l = 1, \dots, L$, where L is the number of coils, $\boldsymbol{n}_l \in \mathbb{C}^M$ are mutually uncorrelated complex white Gaussian noise contributions, $\boldsymbol{A} \in \mathbb{C}^{MxN}$ is the system matrix which encodes the Fourier matrix and the coil sensitivities, and $\boldsymbol{y}_l \in \mathbb{C}^M$ are the k-space data in the l-th coil [1]. We search for the reconstruction $\boldsymbol{x}$ as that minimizes the l_2 norm $E(\boldsymbol{x}) = \|\boldsymbol{y} - \boldsymbol{A}\boldsymbol{x}\|_2$ with $\boldsymbol{y} = [\boldsymbol{y}_1^T, \boldsymbol{y}_2^T, \dots, \boldsymbol{y}_L^T]^T$, and adheres to the parametric form of $\boldsymbol{x}_{dis}$. Because this problem has no closed-form solution, we resort to an iterative algorithm which combines a penalized l_2 reconstruction with an internal Bayesian segmentation using a Gaussian Mixture Model (GMM) [2].

3) Iterative algorithm: The iterative algorithm is defined as $\boldsymbol{x}^{(t+1)} = \arg\min_{\boldsymbol{x}} \left\{E(\boldsymbol{x}) + \left\|\boldsymbol{W}^{(t)}\left(\boldsymbol{x} - \mathcal{P}^{(t)}\{\boldsymbol{x}^{(t)}\}\right)\right\|_2\right\}$, with $\boldsymbol{x}^{(0)} = \arg\min_{\boldsymbol{x}} E(\boldsymbol{x})$, $\boldsymbol{W}^{(t)}$ a weighting diagonal matrix and $\mathcal{P}^{(t)}\{.\}$ is a Bayesian segmentation operator, which for each input image constructs its partially discrete version. The solution $\boldsymbol{x}^{(t+1)}$ balances minimizing $E(\boldsymbol{x})$ and being close to $\mathcal{P}^{(t)}\{\boldsymbol{x}^{(t)}\}$. The penalty term added to the common l_2 reconstruction, controlled by $\boldsymbol{W}^{(t)}$ and termed *discreteness error,* progressively imposes the partial discreteness structure in the solution. The Bayesian segmentation operator $\mathcal{P}^{(t)}\{.\}$ is constructed by fitting a K components GMM to the magnitude of $\boldsymbol{x}^{(t)}$, and then applying Otsu's thresholding algorithm on the probabilistic image defined as $\boldsymbol{x}_{prob} = \sum_{k \in I} \boldsymbol{p}_k^{(t)} \hat{\rho}_k + \sum_{k \notin I} \boldsymbol{p}_k^{(t)} \circ \boldsymbol{x}^{(t)}$, where $\boldsymbol{p}_k^{(t)}$ are the temporally regularized probability maps and $\hat{\rho}_k$ are the means of the classes, both obtained from the GMM. To create $\boldsymbol{x}_{prob}$, it is assumed that classes that belong to I can be identified. The weighting matrix $\boldsymbol{W}^{(t)}$ determines the *discreteness error* probability in different regions. During initial iterations, we set the diagonal entries of $\boldsymbol{W}^{(t)}$ equal to the probability map of the class with the lowest mean (background), because initially our belief of a good classification for the rest of the classes is doubtful. Therefore, the *discreteness error* should not have influence outside of the background. As the algorithm evolves, $\boldsymbol{W}^{(t)}$ could be redefined by including probability maps of the other classes**.** The algorithm stops when the Frobenius norm of $\boldsymbol{W}^{(t+1)} - \boldsymbol{W}^{(t)}$ is below a certain tolerance level. A schematic diagram of the Bayesian segmentation operator is shown in Fig.2. We have tested the partial discreteness prior and the iterative algorithm using MRI breast implant simulated data (Fig.1), which shows the implant rupture. A smoothly varying phase was added to the image and the k space data was synthetized using an equiangular radial scheme with N_{spokes} spokes and 256 samples per spoke. Single-coil acquisition was considered. Complex white Gaussian noise was added leading to an SNR=100 defined as in *Sutton et al.* [1]. The proposed algorithm was run with $K = 3$ and $I = \{1,3\}$, where $k = 1$ and $k = 3$ represent the classes with highest (breast implant) and lowest (background) mean, respectively. The phase was fixed after its estimation from $\boldsymbol{x}^{(0)}$. After five iterations, the probability maps of breast implant and breast tissue were used to update the weighting matrix. Our method was compared to the conjugate gradient (CG) method with smoothness and Total Variation (TV) priors, both implemented with the Impatient Toolbox [3]. After reconstruction, implant contour detection was accomplished on the extracted implant. For the images obtained with the CG method, the implant was extracted after applying Otsu's method. Segmentation based metrics such as the relative number of misclassified pixels (rNMP) [4] and the Dice coefficient [5] were calculated for the implant class and for N_{spokes} between 20 and 95.

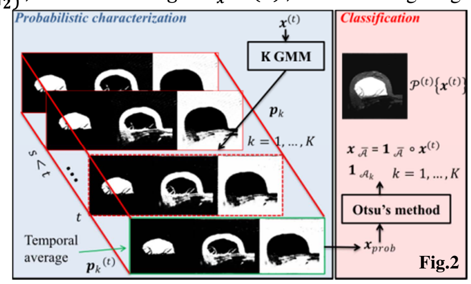

Fig.2

RESULTS: As can be observed from Fig. 3, our proposed algorithm (Fig. 3(c)) allows for substantially better reconstruction and consequently a more accurate contour detection of implant rupture, compared to the other methods (see Fig.3(a) and Fig.3(b)). Moreover, Fig. 4 shows substantially better quantitative results for both metrics and for the complete regime of selected N_{spokes} values.

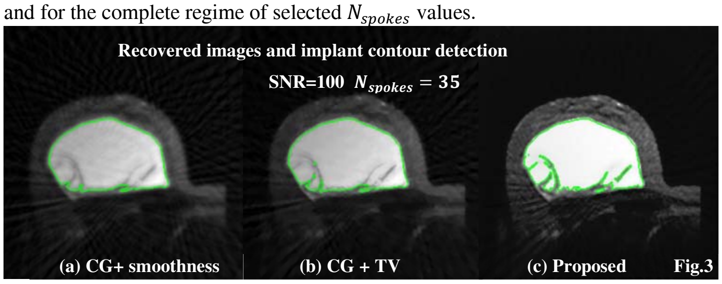

Fig.3

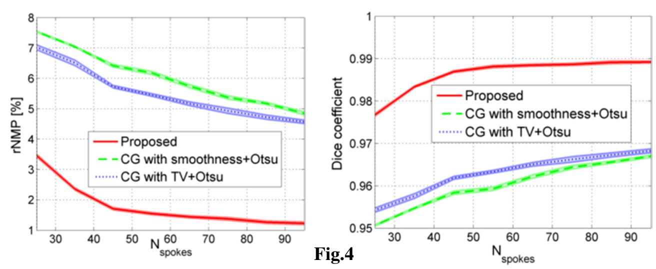

Fig.4

CONCLUSIONS: When the conditions for the partial discreteness assumption hold, the inclusion of the proposed prior in undersampled data scenarios produces more detailedly restored images compared to state-of-the-art methods, and consequently more accurate segmentation is achieved.

REFERENCES: [1] Sutton B.P. *et al.*, IEEE Trans. Med. Imag., 22(2), pp 178-188, [2] Caballero J. *et al.,* MICCAI 2014, 8673, pp 106-113, [3] Gai J. et al., Proc. ISMRM 2012, pp 2250, [4] Segers H. *et al.*, Fund. Inform., 125(3), pp 223-237, [5] Babalola K.O. *et al.* MICCAI 2008, 5241, pp 409-416.